https://doi.org/10.1016/j.compositesb.2017.07.009

Theoretical analysis on the pullout behavior of carbon nanotube at cryogenic environment with the consideration of thermal residual stress

Hei-Lam Ma[a], Kin-tak Lau[b,*], David Hui[c], San-qiang Shi[a], Chi-kin Poon[d]

[a]Department of Mechanical Engineering, The Hong Kong Polytechnic University, Kowloon, Hong Kong

[b]Faculty of Science, Engineering and Technology, Swinburne University of Technology, Melbourne, VIC 3122, Australia

[c]Department of Mechanical Engineering, University of New Orleans, New Orleans, LA70148, USA

[d]Automotive and Electronics Division, Hong Kong Productivity Council, HKPC Building, 78 Tat Chee Avenue, Kowloon, Hong Kong

[*]Corresponding author, e-mail: aklau@swin.edu.au

Abstract

A numerical fiber pullout model tailored for carbon nanotube (CNT) reinforced polymer composites is developed based on some classical models, to evaluate the effect of low temperature environment and other parameters to the stress distribution and stress transfer efficiency in CNT/polymer composites. It is assumed that there are no

bonding between CNTs and polymer so only frictional slip occurs in the interface. Results show that the required axial stress to pull out a straight CNT at cryogenic temperature is more than 6 times greater than that required at room temperature. Some other parameters, such as the length of CNT and the modulus of polymer, also influence the stresses in the CNT/polymer model. The model is also applied to coiled carbon nanotubes (CCNTs) which are newly-developed carbon nanotubes with a helical configuration. At cryogenic temperature, a greater stress is required to pull out a CCNT than a straight CNT, especially in the case when the pitch angle of CCNT is less than 60°. Hence, the stress transfer in CCNT/polymer composites is better than that in straight CNT/polymer composites.

Keywords: A. Particle-reinforcement; B. Fiber/matrix bond, Residual/internal stress; C. Numerical analysis; Cryogenic

1. Introduction

The use of carbon nanotube (CNT) reinforced polymer composites as structural parts in the aerospace industry has been a cutting-edge technology in recent years. According to some technical reports published by NASA [1, 2], using CNT/polymer composites will be the new weight-saving solution. The high specific strength to weight ratio and electrical conductive properties of CNTs make CNT/polymer composites

suitable for many aerospace structures [3, 4]. CNTs are also incorporated into carbon fiber/polymer composites to improve their electrical and thermal conductivity, which are very important properties for dissipating lighting energy [2, 5].

However, extremely low temperature condition will be encountered by these composite aerospace structures during their service in the low earth orbit. The temperature can be down to the cryogenic condition which is $-150℃$ or lower [6, 7]. As the coefficient of thermal expansion of polymer is very much greater than that of CNT, a huge thermal stress will be built up when the composite experiences a temperature change from room temperature to cryogenic temperature. Previous experimental results demonstrated that this thermal residual stress significantly affected the mechanical properties of CNT/polymer composites by enhancing the interfacial properties between CNT and polymer [8, 9]. Yet, to the best knowledge of the authors, there are no existing numerical models that can verify the importance of this stress, especially for CNT/polymer composites, and express it quantitatively. Therefore, it is essential to develop a numerical model with the consideration of this thermal residual stress.

The classical fiber pullout model developed by Zhou et al. [10] has been used to predict the stress distribution along different solid fibers in a single fiber pullout test for

many years [11, 12]. The model accounts for the interfacial properties of the composite including the radial stress due to thermal contraction during curing and also the radial stress acting on fiber due to the difference in Poisson's ratio. In most cases, the matrix has a greater coefficient of thermal expansion then fiber. During curing, matrix contracts at a greater extend then fiber so thermal stress will be induced onto fiber. Similarly, the Poisson's ratio of matrix is usually greater than fiber so a radial clamping force will be induced onto fiber during loading. These two radial compressive stresses significantly affect the interfacial properties. Zhou et al. developed a numerical expression for the radial stress due to the difference in Poisson's ratio but only represents the radial stress due to thermal contraction by a constant q_o.

Chai et al. [13] proposed a fiber push-out model based on the model developed by Zhou et al. Instead of just expressing the thermal residual stress by a constant, a numerical expression relating the material properties to the stress was set up by their team to calculate the thermal residual stress. This expression can also be used to calculate the thermal residual stress built up during conditioning from room temperature to cryogenic temperature in the current problem. The composite is assumed to be placed in cryogenic environment for a long period of time before performing the pullout test in the same environment, so thermal residual stresses are built up before the test. Both the

models developed by Zhou et al. and Chai et al. are for solid fiber only. They cannot be directly used for shell fibers like CNTs. Therefore, modifications are needed.

Besides, the models proposed by Zhou et al. and Chai et al. consider three different interfaces between fiber and matrix including fully bonded, partially bonded and fully debonded. The main assumption for a bonded interface is that fiber and matrix should be perfectly bonded, which is not a common phenomenon in a CNT/polymer composite. For this reason, the whole CNT is assumed to be fully debonded in the current model.

The present study aims to develop a fiber pullout model tailored for CNT/polymer composites based on the classical models for solid fibers. The thermal residual stress due to cryogenic testing environment is taken into consideration and its effects to the overall stresses in the composite are evaluated. This model is also used to study the effect of some physical and geometrical parameters, such as CNT weight percentage and length, to the stresses in the composite at cryogenic environment. Though only CNT/polymer composites are investigated in the present study, the model can literally be used for all hollow fiber reinforced composites.

Coiled multi-walled carbon nanotube (CCNT) is a newly-developed kind of carbon nanotube with a helical configuration. Figure 1 shows a scanning electron microscope (SEM) image of CCNTs [9]. In both room temperature and cryogenic temperature,

experimental results revealed that CCNTs exhibited better reinforcing efficiency with polymer matrix than straight multi-walled carbon nanotubes (MWNTs) [9, 14]. As CCNT/polymer composites are new to researchers, there are very limited studies that quantitatively predict their mechanical behaviors, especially at low temperatures [15]. The straight CNT pullout model developed is also used to predict the effect of the pitch angle of coil to the stresses in CCNT/polymer composite in a fiber pullout test. The results in both room temperature and cryogenic temperature are compared.

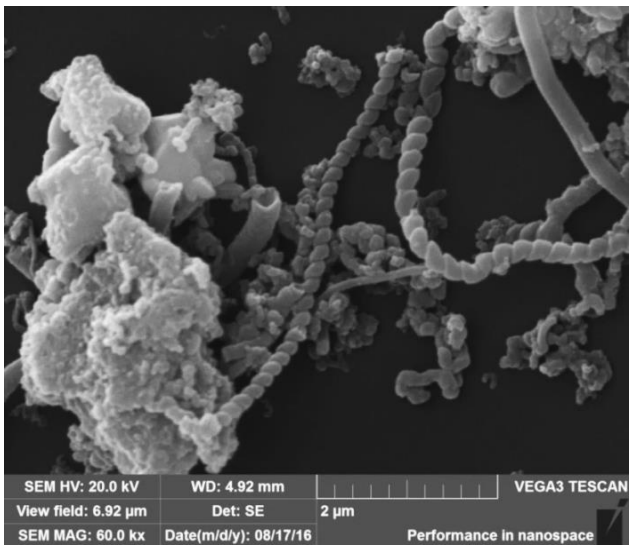

Fig. 1. SEM image of CCNTs [9]

2. Theory

2.1 Geometry of the model

Figure 2 shows a schematic diagram of the CNT pullout model used in the current study. A straight CNT with an outer radius a is embedded into a cylindrical matrix with radius b. The CNT and the matrix are concentric along the z-axis. The total length of

the composite is L. The CNT is considered as a number of concentric hollow tubes. p_o, h and d correspond to the non-relaxed radius of the innermost wall, the thickness of one wall and the spacing between layers [16]. Figure 3 shows a schematic diagram of a MWNT. The number of walls is represented by N. When $N = 1$, it is a single-walled carbon nanotube (SWNT). The outer radius a of a CNT can be expressed as:

$$a = p_0 + d(N - 1) \quad (1)$$

Yet, CNTs have end caps. In real CNT/polymer composites, only the outermost wall is in contact with matrix. According to Lau et al. [17], the inner walls do not have much contribution to the load carrying capacity since the Van der Waals force between walls is very weak. Thus, a MWNT can be treated as a SWNT with larger outer radius. The effective cross-sectional area A_{eff} of the CNT can then be given by

$$A_{eff} = 2\pi h[p_0 + d(N - 1)] \quad (2)$$

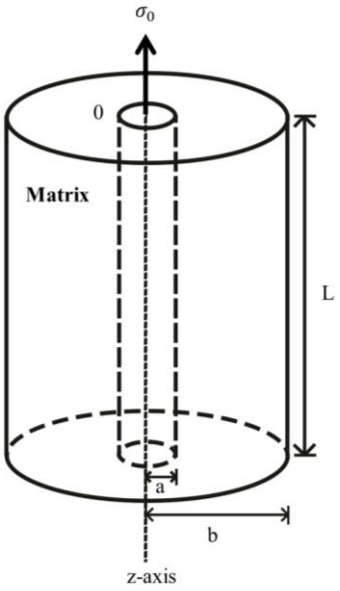

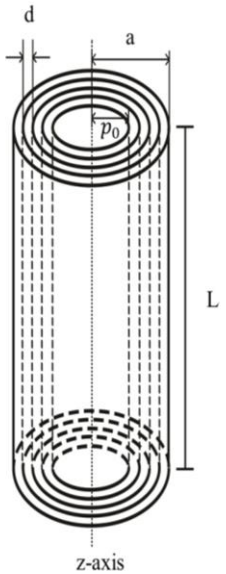

Fig. 2. Schematic diagram of the CNT pullout model

Fig. 3. Schematic diagram of a MWNT

2.2 Governing differential equations

During CNT pullout, the axial stress and interfacial shear stress on both CNT and matrix should be at equilibrium. The differential equations for the axial stress of CNT $\sigma_{NT}(z)$ and axial stress of matrix $\sigma_m(z)$ can therefore be written as:

$$\frac{d\sigma_{NT}(z)}{dz} = -\frac{2\pi a}{A_{eff}}\tau(z) \quad (3)$$

$$\frac{d\sigma_m(z)}{dz} = \frac{2a}{(b^2-a^2)}\tau(z) \quad (4)$$

where $\tau(z)$ is the interfacial shear stress. Let γ be the area ratio of CNT to matrix, i.e.:

$$\gamma = \frac{A_{eff}}{\pi(b^2-a^2)} \quad (5)$$

The axial stress of matrix $\sigma_m(z)$ can then be simplified into:

$$\frac{d\sigma_m(z)}{dz} = \frac{2\pi a}{A_{eff}}\gamma\,\tau(z) \quad (6)$$

2.3 Radial stresses

According to Zhou et al., frictional slip occurs in the fully debonded interface. The stress transfer at the interface is assumed to be governed by Coulomb's friction law with μ being the coefficient of friction. The interfacial shear stress $\tau(z)$ can then be expressed by:

$$\tau(z) = \mu q(z) \quad (7)$$

where $q(z)$ refers to the interfacial radial stress. In the present problem, $q(z)$ is assumed to be composed of the radial stress due to residual thermal stress q_0 and the radial stress due to Poisson's effect $q_a(z)$ only. Hence:

$$\tau(z) = -\mu[q_0 - q_a(z)] \quad (8)$$

q_0 is a constant as the temperature of the testing environment is constant throughout the whole CNT pullout process. As suggested by Chai et al., it can be numerically expressed in terms of the Young's moduli of matrix E_m and CNT E_{NT}, the coefficients of thermal expansion of matrix α_m and CNT α_{NT}, the Poisson's ratios of matrix v_m and CNT v_{NT}, the change in temperature and the geometrical factors of the model. In order to take the low temperature environment into consideration, the change in temperature is expanded into two constants namely the change in temperature during curing ΔT_{curing} and conditioning $\Delta T_{conditioning}$, i.e.:

$$q_0 = \frac{E_m(\alpha_m - \alpha_{NT})(\Delta T_{curing} + \Delta T_{conditioning})}{\alpha(1 - v_{NT}) + (1 + 2\gamma + v_m)} \quad (9)$$

Since the change in temperature during curing and conditioning are both negative in the present case, q_0 must be negative which represents a radial compressive stress.

The stress due to Poisson's effect $q_a(z)$ varies along the z-axis as it is related to the axial stress of CNT and matrix. It was calculated according to the general relationships between stress and strain by Zhou et al.:

$$q_a(z) = \frac{\alpha v_f \sigma_{NT}(z) - v_m \sigma_m(z)}{\alpha(1-v_{NT})+(1+2\gamma+v_m)} \quad (10)$$

where α is the Young's modulus ratio of matrix E_m to CNT E_{NT}. Inserting equation (9) and (10) into (8), the differential equations for the axial stress of CNT $\sigma_{NT}(z)$ and matrix $\sigma_m(z)$ become:

$$\frac{d\sigma_{NT}(z)}{dz} = -\frac{2\pi a\mu}{A_{eff}}\left[-\frac{E_m(\alpha_m-\alpha_{NT})(\Delta T_{curing}+\Delta T_{conditioning})}{\alpha(1-v_{NT})+(1+2\gamma+v_m)} + \frac{\alpha v_f \sigma_{NT}(z) - v_m \sigma_m(z)}{\alpha(1-v_{NT})+(1+2\gamma+v_m)}\right] \quad (11)$$

$$\frac{d\sigma_m(z)}{dz} = \frac{2\pi a\gamma\mu}{A_{eff}}\left[-\frac{E_m(\alpha_m-\alpha_{NT})(\Delta T_{curing}+\Delta T_{conditioning})}{\alpha(1-v_{NT})+(1+2\gamma+v_m)} + \frac{\alpha v_f \sigma_{NT}(z) - v_m \sigma_m(z)}{\alpha(1-v_{NT})+(1+2\gamma+v_m)}\right] \quad (12)$$

2.4 Solutions

In a typical CNT pullout test, an axial stress σ_0 is applied onto the CNT at $z = 0$ while the matrix is free of stress. At $z = L$, the CNT is free of stress while an axial stress of $\gamma\sigma_0$ is applied onto the matrix. Thus, the boundary conditions for the present problem are $\sigma_{NT}(0) = \sigma_0$, $\sigma_m(0) = 0$, $\sigma_{NT}(L) = 0$ and $\sigma_m(L) = \gamma\sigma_0$.

By solving the differential equations with the boundary conditions, the following solutions describing the stresses in a CNT pullout test at low temperature can be obtained:

$$\sigma_{NT}(z) = \sigma_0 - \omega(\bar{\sigma} - \sigma_0)\left[e^{\lambda z} - 1\right] \quad (13)$$

$$\sigma_m(z) = \gamma\omega(\bar{\sigma} - \sigma_0)\left[e^{\lambda z} - 1\right] \quad (14)$$

$$\tau(z) = \frac{A_{eff}\lambda\omega}{2\pi a}(\bar{\sigma} - \sigma_0)e^{\lambda z} \quad (15)$$

where

$$\omega = \frac{\alpha v_f}{\alpha v_f + \gamma v_m} \tag{16}$$

$$\bar{\sigma} = \frac{q_0}{\omega k} \tag{17}$$

$$\lambda = \frac{2\pi a \mu k}{A_{eff}} \tag{18}$$

$$k = \frac{\alpha v_f + \gamma v_m}{\alpha(1 - v_f) + (1 + 2\gamma + v_m)} \tag{19}$$

2.5 Stresses in CCNTs

According to Hao et al., a coiled reinforcement can be modeled as a straight reinforcement that is inclined at every point along its length [18]. The pullout load can be decomposed into a parallel pullout force and also a perpendicular bending force which changes the direction of the fiber during pullout [19]. Figure 4 shows the relationship between the stresses and the pitch angle of coil θ in a CCNT/polymer composite.

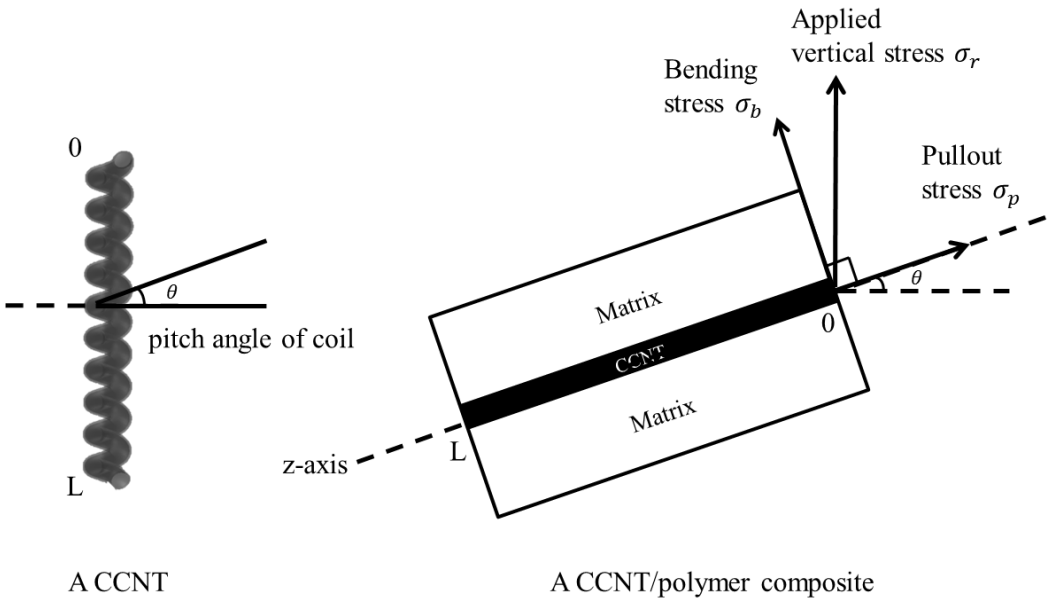

Fig. 4. The relationship between the stresses and the pitch angle in a CCNT/polymer

composite

Let the applied vertical stress to pullout the CCNT be σ_r, the axial pullout stress be σ_p and the bending stress be σ_b. L is the unwound length of the CCNT. The applied axial stress σ_0 at z=0 (boundary condition) from the straight CNT pullout model in section 2.1-2.4 is then the axial pullout stress σ_p of CCNT. σ_0 can be expressed in terms of the applied vertical stress σ_r and the pitch angle θ:

$$\sigma_r = \frac{\sigma_o}{sin\theta} \tag{20}$$

The total interfacial shear stress of a spiral fiber reinforced composite τ_c at the exit point (z=0) composes of two stresses, including the interfacial shear stress due to radial compression τ_r and the interfacial shear stress due to bending compression τ_b at the exit point [20], i.e.

$$\tau_c = \tau_r + \tau_b \tag{21}$$

τ_r is the interfacial shear stress of straight CNT. According to the previous pullout model, τ_r equals to zero at z=0. τ_b is the interfacial shear stress due to the point stress σ_b which acts only on the exit point. It moves along the axial position of CNTs during pullout. By Coulomb's law of friction, τ_b can be expressed in terms of the coefficient of friction between CCNT and matrix μ, the applied vertical stress σ_r and the pitch angle θ:

$$\tau_b = \mu\sigma_b = \mu\sigma_r cos\theta \tag{22}$$

Since $\tau_r = 0$ at z=0, by substituting equation 20 and 22 to 21, the interfacial shear stress of a CCNT/polymer composite is then:

$$\tau_c = \mu\sigma_o cot\theta \quad (23)$$

The only unknowns in equations 20 and 23 are the coefficient of friction, the pitch angle and the applied axial stress for straight CNT. The first two are material constants. The applied axial stress can be obtained from the straight CNT pullout model and it varies with temperature. Hence, the stresses in a CCNT/polymer composite at low temperature can be predicted easily with these equations.

3. Results and discussion

Graphs are plotted according to the expressions obtained in section 2 to analyze the effect of different physical parameters to the stresses in composites. The material constants used are from some previous works done by other researchers [14, 21-24] and also experiments done by our team. Table 1 shows a list of material constants while Table 2 shows the general geometric parameters of the CNT used in the current study.

Table 1 Material constants

Item		**Value**
Young's Modulus (GPa)	Matrix at 293K $E_{m,293K}$	2.80
	Matrix at 123K $E_{m,123K}$	4.40
	Matrix at 100K $E_{m,100K}$	4.70
	Matrix at 77K $E_{m,77K}$	5.00
	Carbon nanotube E_{NT}	1000
Poisson's ratio	Matrix v_m	0.48
	Carbon nanotube v_{NT}	0.2

Coefficient of thermal expansion (K^{-1})	Matrix α_m	$6.5x10^{-5}$
	Carbon nanotube α_{NT}	$0.1x10^{-5}$
Coefficient of friction μ		0.48
Change in temperature during curing ΔT_{curing} (K)		-40

Table 2 General geometric parameters of carbon nanotube

Item	**Value**
Thickness of one wall h (m)	$6.17x10^{-11}$
The non-relaxed radius of the inner most wall p_0 (m)	$6.94x10^{-9}$
Spacing between layers d (m)	$3.4x10^{-10}$

3.1 Straight carbon nanotubes

3.1.1 The effect of cryogenic temperature environment

To evaluate the effect of cryogenic temperature environment to a straight CNT/polymer composite in a pullout test, the axial stress along CNT $\sigma_{NT}(z)$ and the interfacial shear stress in the CNT/polymer interface $\tau(z)$ are plotted with respect to the dimensionless axial position (z/L) (Figure 5(a) & (b)). Three cryogenic temperatures, 77K, 100K and 123K, are selected. The CNT is assumed to have 10 walls and a length of 2um. The weight percentage of CNT is 1%.

From the graphs, a greater axial stress is required for a greater temperature change from curing to conditioning, i.e. lower testing temperature. The axial stress required to pull out a CNT at liquid nitrogen temperature (77K) is around 6.5 times larger than that required at room temperature (293K). The difference in interfacial shear stress is even more obvious. The interfacial shear stress at the CNT end at 77K is around 8 times

larger than that at 293K which indicates that the clamping force acting on CNT by polymer, due to thermal expansion mismatch, mechanically improves the interfacial bonding.

The characteristic length for stress transfer has longed been an important parameter for evaluating the fiber pullout behavior in composite materials. It refers to the length where the axial stress increases from zero dramatically to a saturated value while the interfacial shear stress decreases dramatically and vanishes [25]. The shorter the characteristic length, the more efficient the stress transfer is, when efficiency is in terms of length [26]. From Figure 5(a) & (b), the characteristic length for stress transfer is the same for all temperatures. Hence, it can be concluded that low temperature testing environment increases the required stress to pull out a CNT but has no effect to the stress transfer efficiency with respect to CNT length.

(a) (b)

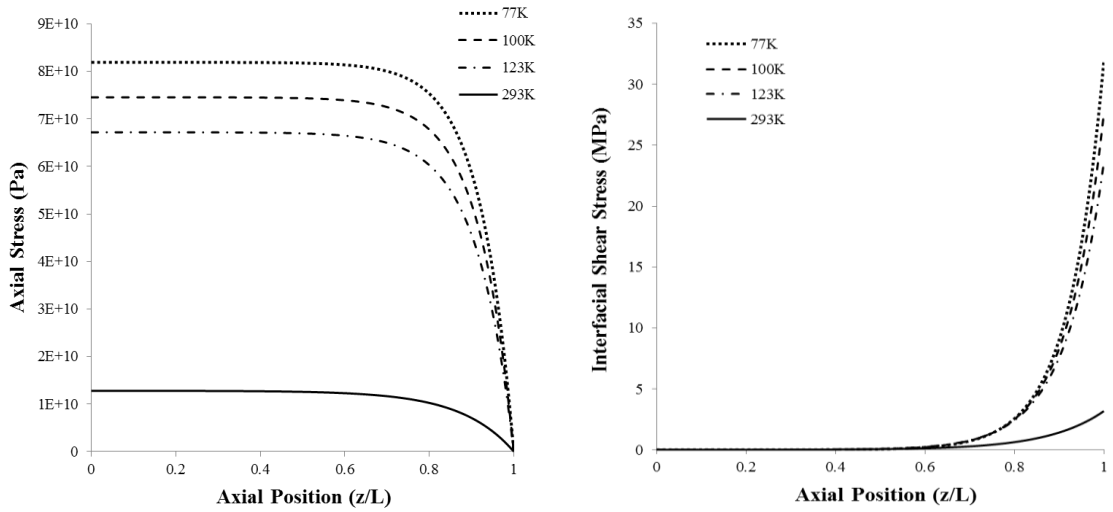

Fig. 5. (a) Axial stress along CNT and (b) interfacial shear stress with different testing temperatures

3.1.2 The effect of CNT weight percentage

The effect of CNT weight percentage to the mechanical properties of CNT/polymer composites has been a hot research direction for scholars [27-31]. In the current model, different weight percentages of CNTs are defined as different radii of the cylindrical matrix. The greater the weight percentage of CNTs, the smaller the radius of the cylindrical matrix is. Figure 6(a) & (b) shows the axial stress along CNT and the interfacial shear stress with different weight percentage of CNTs at 77K. The graphs show that for different weight percentages, the axial stress required to pullout the CNT from matrix remains nearly constant and the interfacial shear stress is similar along nearly the whole fiber length. These phenomena were also observed in previous literatures [22, 32].

There is much variation in the characteristic length for stress transfer when different weight percentages of CNT are used. The characteristic length decreases with increasing weight percentage which indicates that the stress transfer efficiency in terms of CNT length is higher in greater weight percentages. The optimal weight percentage is around 7% for the present case. At this percentage, the stiffness of the slope near the

CNT end almost reaches a maximum. Further increasing the percentage will have nearly no effect on the stress transfer efficiency.

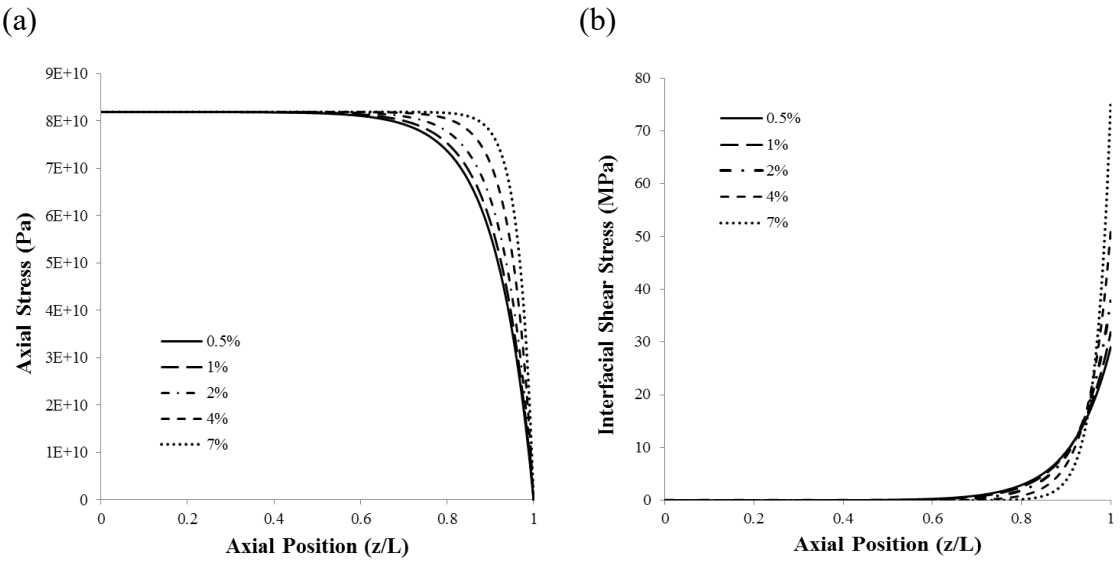

Fig. 6. (a) Axial stress along CNT and (b) interfacial shear stress with different CNT weight percentages at 77K

3.1.3 The effect of CNT wall number

Aerospace structure designers utilize different kinds of CNTs including single-walled CNTs, double-walled CNTs and few-walled CNTs to make nanocomposites [1, 2, 33-35]. As mentioned in the previous session, only the outermost wall of CNT carries load in a CNT/polymer composite. Different number of walls affects the outer radius of CNT, which is governed by equation (1). The greater the wall number, the greater the outer radius of CNT is. Besides, the carbon content in one CNT increases with increasing number of walls. Thus, using CNTs with a smaller wall number increases the volume fraction of CNT in a CNT/polymer composite for a given

weight percentage (1%). This is represented by a smaller radius of the cylindrical matrix in the current model.

The trend shown in the graphs for different CNT wall number at 77K (Figure 7(a) & (b)) is similar to that shown in section 3.1.2. The required axial stress to pull out the CNT from matrix is the same for all kinds of CNTs. Yet, the characteristic length for stress transfer increases with increasing wall number. The stress transfer efficiency is the highest in single-walled CNT since it has the greatest surface area to volume ratio and also, the total number of CNTs in a single-walled CNT/polymer composite is the greatest for the same CNT weight percentage.

(a) (b)

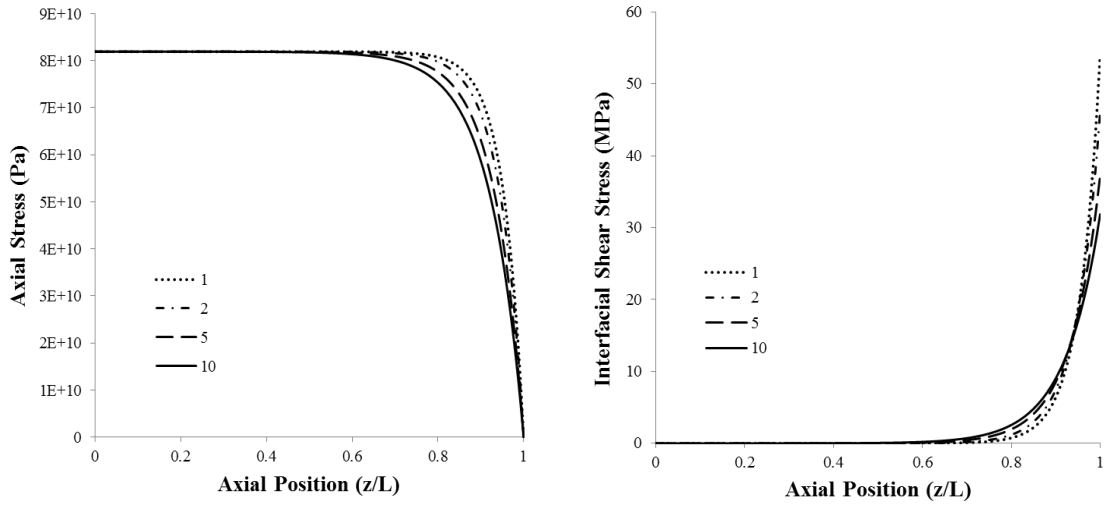

Fig. 7. (a) Axial stress along CNT and (b) interfacial shear stress with different CNT wall number at 77K

3.1.4 The effect of CNT length

Different CNT lengths (0.5, 1, 2, 4, 5 um) are applied to the numerical model to study their effect to the stresses in the composite at 77K. In this case, the CNT was assumed to have 10 walls and the weight percentage is 1%. Figure 8(a) & (b) show the stresses. In general, a greater axial stress is required to pull out a CNT with longer length. The interfacial shear stress decreases with increasing CNT length which is similar to the behavior observed by Jia et al. and Duncan et al. [36, 37] for room temperature testing environment.

From the graphs, the characteristic length for stress transfer increases with decreasing CNT length. For a CNT length of 0.5um, the saturation point cannot even be attained. Stress cannot be fully transferred between CNT and polymer so the CNT will be pulled out very easily. To optimize the stress transfer efficiency, the optimal CNT length was found. It is around 5um for the present case, where the characteristic length for stress transfer is the shortest. Further increasing the length will have nearly no effect to the stresses in the composite.

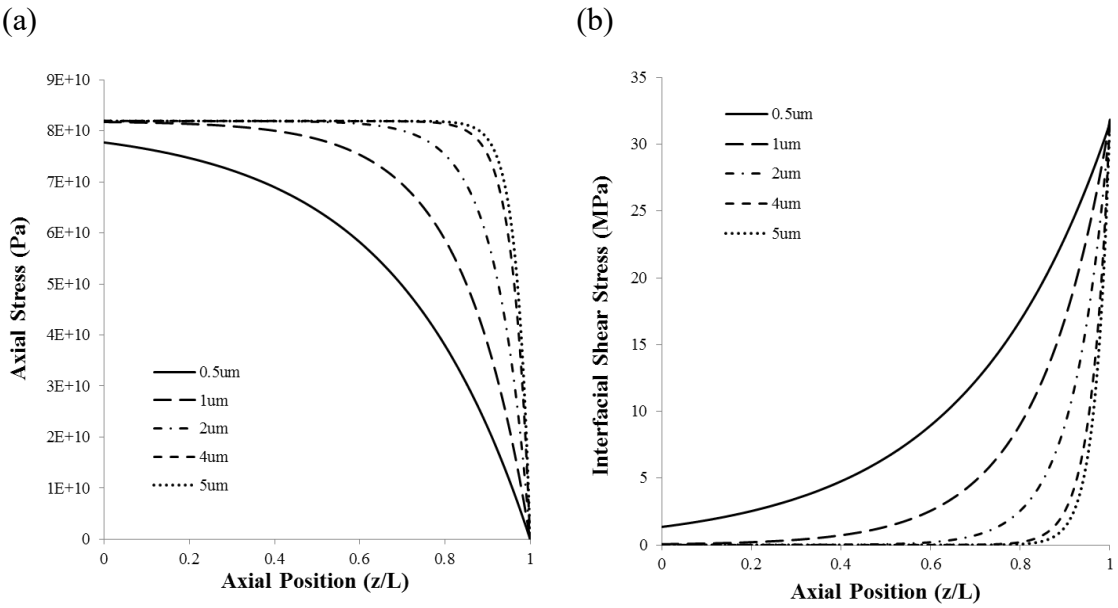

Fig. 8. (a) Axial stress along CNT and (b) interfacial shear stress with different CNT lengths at 77K

3.1.5 The effect of polymer modulus

Many different kinds of polymer matrix are used for fabricating aerospace composites, including phenolic, polyester and epoxy. Their elastic moduli at room temperature range from 0.8GPa to 3.2GPa while in cryogenic temperature; they are approximately three times greater [38-40]. The variations in axial stress along CNT and interfacial shear stress at 77K, when different polymer moduli are used, are shown in Figure 9 (a) & (b). The axial stress required to pull out a CNT is nearly the same for all moduli, yet, the characteristic length for stress transfer varies. Composites with a smaller matrix modulus show a longer characteristic length which means lower stress transfer efficiency. The optimal matrix modulus is approximately 8GPa in the present

case and further increasing the modulus will have very small effect on the fiber pullout behavior of CNT/polymer composites.

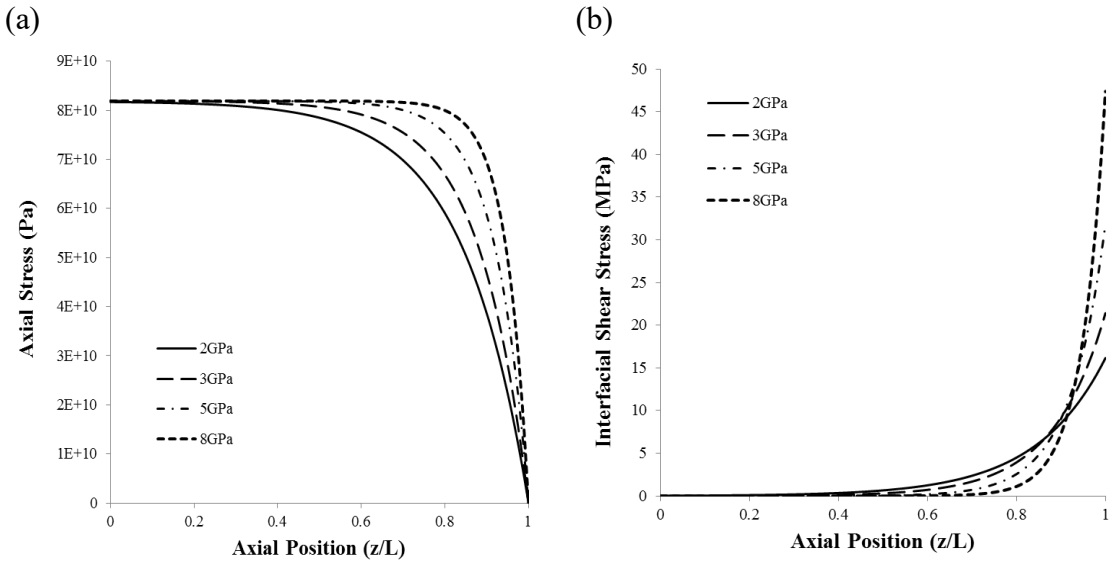

Fig. 9. (a) Axial stress along CNT and (b) interfacial shear stress with different polymer modulus at 77K

3.2 Coiled carbon nanotubes

As mentioned in section 2.5, a CCNT can be considered as a straight CNT with an inclination which is characterized by the pitch angle of coil. To understand the effect of pitch angle to the stresses in CCNT/polymer composites at low temperature, graphs of the required vertical stress and interfacial shear stress at the exit point versus pitch angle are plotted (Figure 10 (a) & (b)). A pitch angle of 90° corresponds to the case of straight CNT. In general, the stresses at cryogenic temperature are higher than that at room temperature, which is consistent with the results for straight CNT as shown in Figure 5.

At both temperature conditions, the required vertical stress to pullout the CCNT does not change much as the pitch angle decreases from 90° to 60°. When the pitch angle is further decreased, the two curves depart from each other, first gradually, then drastically. That means a significantly greater force is required to pullout a CCNT than a straight CNT at cryogenic temperature, if the pitch angle is small enough. The interfacial shear stress at the exit point (z=0) behaves similarly, except that both curves start from zero at 90°. The gap between them becomes greater and greater as the pitch angle decreases. The graphs indicate that at low temperature condition, CCNTs with small pitch angle are more difficult to be pulled out than straight CNTs. Previous experimental results showed that CCNT/polymer composites were much stiffer than straight CNT/polymer composites at cryogenic condition [9]. This phenomenon can be well-explained by the current model. Since CCNTs are more difficult to be pulled out, the stress transfer efficiency between CCNT/polymer composites is better than that in straight CNT/polymer composites. It consequently leads to a greater stiffness in CCNT/polymer composites. Hence, CCNTs are very effective reinforcement for polymers to be servicing at cryogenic temperatures.

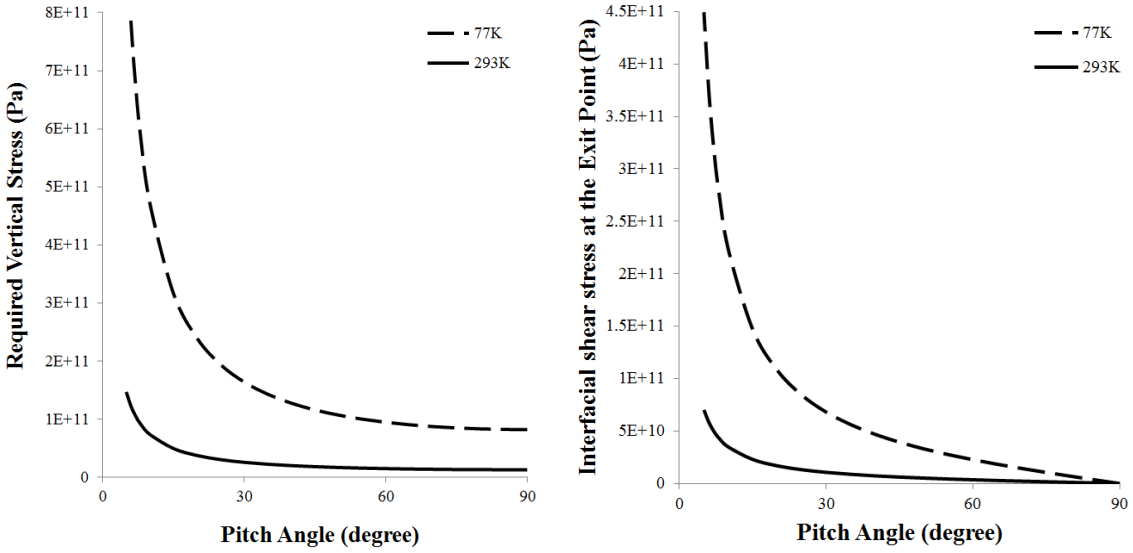

Fig. 10. (a) Required vertical stress versus pitch angle of CNT and (b) interfacial shear stress at z=0 versus pitch angle of CCNT

Conclusion

A numerical fiber pullout model tailored for CNT/polymer composites is developed to evaluate the effect of low temperature testing environment and other parameters to the stress distribution and stress transfer efficiency in composites. It is assumed that there are no bonding between CNTs and polymer. Only frictional slip occurs in the interface. Graphs on the axial stress of straight CNTs and the interfacial shear stress between CNT and matrix are plotted. Results from numerical analysis on straight CNTs show that the required axial stress to pull out a CNT at cryogenic temperature is more than 6 times greater than that required at room temperature. The model is also applied to CCNTs. It can be seen from the graphs that at cryogenic temperature, a greater stress is required to pull out a CCNT than a straight CNT,

especially in the case where the pitch angle of CCNT is less than 60°. Hence, the stress transfer efficiency in CCNT/polymer composites is better than that in straight CNT/polymer composites.

Acknowledgement

The authors are grateful for the support provided by the Hong Kong Polytechnic University Grant and the Swinburne University of Technology Research Grant to this project.

References

1. Siochi EJ, Kim JW, Sauti G, Cano RJ, Wincheski RA, Ratcliffe JG, Czabaj M, Jensen BD, Wise KE. High volume fraction carbon nanotube composites for aerospace applications. NASA Technical Reports. Oct 26, 2015, Document ID: 20160006413.
2. Cano RJ, Kang JH, Grimsley BW, Ratcliffe JG, Siochi EJ. Properties of multifunctional hybrid carbon nanotube/carbon fiber polymer matrix composites. NASA Technical Reports. May 22, 2016, Document ID: 20160009128.
3. Gohardani O, Elola MC, Elizetxea C. Potential and prospective implementation of carbon nanotubes on next generation aircraft and space vehicles: A review of current and expected applications in aerospace sciences. Progress in Aerospace Sciences 2014;70;42-68
4. Pal G, Kumar, S. Modeling of carbon nanotubes and carbon nanotube-polymer composites. Progress in Aerospace Sciences 2016;80;33-58
5. De Rosa IM, Sarasini F, Sarto MS, Tamburrano A. EMC impact of advanced carbon fiber/carbon nanotube reinforced composites for next-generation aerospace applications. IEEE Transactions on Electromagnetic Compatibility 2008;50(3);556-563
6. Shao Y, Xu F, Liu W, Zhou M, Li W, Hui D, Qiu Y. Influence of cryogenic treatment on mechanical and interfacial properties of carbon nanotube fiber/bisphenol-F epoxy composite. Composites Part B 2017 doi: 10.1016/j.compositesb.2017.05.077
7. Ajaja J, Barthelat F. Damage accumulation in a carbon fiber fabric reinforced cyanate ester composite subjected to mechanical loading and thermal cycling. Composites Part B 2016;90;523-529
8. Ma HL, Jia Z, Lau KT, Leng J, Hui D. Impact properties of glass fiber/epoxy composites at cryogenic environment. Composites Part B 2016;92;210-217
9. Ma HL, Jia Z, Lau KT, Li X, Hui D, Shi SQ. Enhancement on mechanical strength of adhesively-bonded composite lap joints at cryogenic environment using coiled carbon nanotubes. Composites Part B 2017;110;396-401
10. Zhou LM, Mai YW, Baillie C. Interfacial debonding and fibre pull-out stresses Part V A methodology for evaluation of interfacial properties. Journal of Materials Sciences 1994;29;5541-50
11. Poon CK, Zhou LM, Jin W, Shi SQ. Interfacial debond of shape memory alloy composites. Smart Materials and Structures 2005;14;N29-N37
12. Quek MY. Stress transfer at a partially bonded fibre/matrix interface. International Journal of Adhesion and Adhesives 2002;22(4);303-310
13. Chai YS, Mai YW. New analysis on the fiber push-out problem with interface

roughness and thermal residual stresses. Journal of Materials Science 2001;36;2095-104
14. Lau KT, Lu M, Liao K. Improved mechanical properties of coiled carbon nanotubes reinforced epoxy nanocomposites. Composites Part A 2006;37;1837-40.
15. Khani N, Yildiz M, Koc B. Elastic properties of coiled carbon nanotube reinforced nanocomposte: A finite element study. Materials and Design 2016;109;123-32
16. Lau KT. Interfacial bonding characteristics of nanotube/polymer composites. Chemical Physics Letters 2003;370;399-405
17. Lau KT, Gu Chong, Gao GH, Ling HY, Reid SR. Stretching process of single- and multi-walled carbon nanotubes for nanocomposite applications. Carbon 2004;42;426-428
18. Hao Y, Hao H. Pull-out behavior of spiral-shaped steel fibres from normal-strength concrete matrix. Construction and Building Materials 2017;139;34-44
19. Zhang H, Yu RC. Inclined fiber pullout from a cementitious matrix. Materials 2016;9;800
20. He X, Wang C, Tong L, Li Y, Peng Q, Mei L, Wang R. A pullout model for inclined carbon nanotube. Mechanics of Materials 2012;52;28-39
21. Vodenitcharova T, Zhang LC. Effective wall thickness of a single-walled carbon nanotube. Physical Review B 2003;68;165401
22. Shintani K, Narita T. Atomistic study of strain dependence of Poisson's ratio of single-walled carbon nanotube. Surface Science 2003;532-535;862-868
23. Jia Z, Ma HL, Cheng LK, Lau KT, Hui D. Stress transfer properties of carbon nanotube reinforced polymer composites at low temperature environments. Composites Part B 2016;106;356-365
24. Ahmed KS, Keng AK. Interface characteristics of carbon nanotube reinforced polymer composites using an advanced pull-out model. Computational Mechanics 2014;53;297-308
25. Chen B, Wu PD, Gao H. A characteristic length for stress transfer in the nanostructure of biological composites. Composites Science and Technology 2009;69;1160-1164
26. Andersons J, Leterrier Y, Tornare G, Dumont P, Manson JAE. Evaluation of interfacial stress transfer by coating fragmentation test. Mechanics of Materials 2007;39;834-844
27. Moumen AEI, Tarfaoui M, Lafdi K, Benyahia H. Dynamic properties of carbon nanotubes reinforced carbon fibers/epoxy textile composites under low velocity impact. Composites Part B 2017;125;1-8
28. Chakrabarty A, Cagin T. Thermo-mechanical properties of a piezoelectric polyimide

carbon nanotube composite: Assessment of composite theories. Computational Materials Science 2014;92;185-191
29. Dong S, Zhou J, Hui D, Wang Y, Zhang S. Size dependent strengthening mechanisms in carbon nanotube reinforced metal matrix composites. Composites Part A 2015;68;356-364
30. Hanif WYW, Risby MS, Noor MM. Influence of carbon nanotube inclusion on the fracture toughness and ballistic resistance of twaron/epoxy composite panels. Procedia Engineering 2015;114;118-123
31. Tarfaoui M, Lafdi K, Moumen AE. Mechanical properties of carbon nanotubes based polymer composites. Composites Part B 2016;103;113-121
32. Spanos KN, Georgantzinos SK, Anifantis NK. Investigation of stress transfer in carbon nanotube reinforced composites using a multi-scale finite element approach. Composites Part B 2014;63;85-93
33. Spitalsky Z, Tasis D, Papagelis K, Galiotis C. Carbon nanotube-polymer composites: Chemistry, processing, mechanical and electrical properites. Progress in Polymer Science 2010;35(3);357-401
34. Kim MT, Rhee KY, Lee JH, Hui D, Lau AKT. Property enhancement of a carbon fiber/epoxy composite by using carbon nanotubes. Composites Part B 2011;42;1257-1261
35. Chandra Y, Scarpa F, Adhikari S, Zhang J, Flores EIS, Peng HX. Pullout strength of graphene and carbon nanotube/epoxy composites. Composites Part B 2016;102;1-8
36. Jia Y, Chen Z, Yan W. A numerical study on carbon nanotube pullout to understand its bridging effect in carbon nanotube reinforced composites. Composites Part B 2015;81;64-71
37. Duncan RK, Chen XG, Bult JB, Brinson LC, Schadler LS. Measurement of the critical aspect ratio and interfacial shear strength in MWNT/polymer composites. Composites Science and Technology 2010;70;599-605
38. Bafekrpour E, Simon GP, Naebe M, Habsuda J, Yang C, Fox B. Preparation and properties of composition-controlled carbon nanofiber/phenolic nanocomposites. Composites Part B 2013;52;120-126
39. Manalo AC, Wani E, Zukarnain NA, Karunasena W, Lau KT. Effects of alkali treatment and elevated temperature on the mechanical properties of bamboo-fibre-polyester composites. Composites Part B 2015;80;73-83
40. Huang CJ, Fu SY, Zhang YH, Lauke B, Li LF, Ye L. Cryogenic properties of SiO_2/epoxy nanocomposites. Cryogenics 2005;45;450-454